Biofilm Growth Under Elastic Confinement: Supplementary Material

George T. Fortune, Nuno M. Oliveira, and Raymond E. Goldstein
Department of Applied Mathematics and Theoretical Physics,
University of Cambridge, Cambridge CB3 0WA, United Kingdom
(Dated: December 2, 2021)

We present dimensionless shallow layer scalings that reduce the system of equations describing the full system (2)-(6) in the main text to a pair of coupled differential equations for the height $h(r,t)$ and vertically averaged biomass volume fraction $\langle\phi\rangle(r,t)$ as a function of radial distance r and time t. The deformation $\boldsymbol{\xi}$ is expressed as a function of derivatives of h, utilizing both global biomass volume conservation and a pressure condition at the biofilm interface. The system is closed with boundary conditions for h at the biofilm interface, obtained by extending the framework outside the biofilm to the whole domain and imposing far-field free-beam and zero-pressure conditions.

EXPERIMENTAL

Supplementary information on methods and materials

All experiments reported here used flagella-null cells of *Bacillus subtilis* (NCIB 3610 hag::tet, a gift from Roberto Kolter). Flagellaless cells were preferred because their inability to swim largely avoids contamination of inlets loaded with fresh growth medium in the microfluidic devices, and removes motility as a secondary contribution to biofilm spreading, as in earlier work [S1].

For each experiment, *Bacillus subtilis* cells were streaked from −80°C freezer stocks onto 1.5% agar LB plates and incubated at 37°C for 12 hours. Cells from a single colony were then inoculated in LB Broth (Lennox) at 37°C for 3 hours to obtain cells in the exponential growth phase. These were centrifuged at 2600 rpm for 6 minutes and re-suspended with fresh minimal salts glycerol glutamate (MSgg), the standard biofilm growth medium for *B. subtilis* [S1]. This MSgg medium contained 5 mM potassium phosphate buffer (pH 7.0), 100 mM MOPS buffer (pH 7.0), 2 mM $MgCl_2$, 700μM $CaCl_2$, 50μM $MnCl_2$, 100 μM $FeCl_3$, 1 μM $ZnCl_2$, 2 μM thiamine HCl, 0.5% (v/v) glycerol and 0.5% (w/v) monosodium glutamate.

Cells were then loaded at the center of Y04-D plates linked to the CellASIC ONIX microfluidic platform (EMD Millipore), and were incubated at 30 °C for the duration of each experiment. In this setup, they were confined between a rigid surface (glass) and an elastic sheet (PDMS, 114 μm thick), a distance 6 μm apart. In all experiments we flowed fresh MSgg medium via one inlet, using a pump pressure of 1 psi, corresponding to a mean flow rate of 16 μms^{-1} in the growth chamber [S2–S4]. The subsequent growth of these submerged biofilms was then followed over time with a Zeiss Axio Observer Z1 microscope, connected to a Yokogawa Spinning Disk Confocal CSU and controlled by Zen Blue software. A Zeiss 10 × /0.3 M27 Plan-Apochromat objective lens was used to acquire bright-field images at a rate of 1 frame per minute. These images were analyzed using both the open source image processing package Fiji [S5] and several custom MATLAB scripts utilizing MATLAB's Image Processing Toolbox. In particular, a Sobel edge detector was used to locate the biofilm edge. The experimental biofilms were often frilly with long thin strands of matrix polymer protruding from the biofilm edge. Hence, 2D gaussian filtering using the MATLAB inbuilt function imgaussfilt was used to neglect these strands when identifying where the interface is. In order to fit a circle to the extracted interface a least-squares fit was implemented.

Raw experimental data

Figure S1 gives the corresponding raw data for the experiment given in the montage plot of Figure 3(a) of the main text, showing how in Figure S1(a) the scaled biofilm radius $\mathcal{R}$ and in Figure S1(b) σ_b, a measure of the circularity of the biofilm edge, vary with time, where σ_b satisfies

$$\sigma_b = \mathrm{std}\left(\boldsymbol{r_b} - \mathcal{R}\right)/\mathcal{R}. \tag{S1}$$

Here, $\boldsymbol{r_b}$ is a vector giving the scaled distance of the points on the biofilm edge from the center of the biofilm. As a biofilm grows, it becomes more circular (after an initial increase due to growth around an obstacle σ_b decreases monotonically) but with frillier edges. Furthermore, as shown in the montage plot, interference fringes (Newton rings) are used to gain a qualitative understanding of how the upper PDMS sheet deforms. In particular, the fringes are circular, implying that the sheet deforms asymmetrically and thus evolves consistently with one of the key assumptions of the theoretical model, namely that $h = h(r,t)$ is independent of θ.

Fitting Procedure

Numerical solutions of (S63) predict the evolution of $\mathcal{R}$ as a function of dimensionless time τ, with a single fitted parameter Ξ. To convert back to real time, the

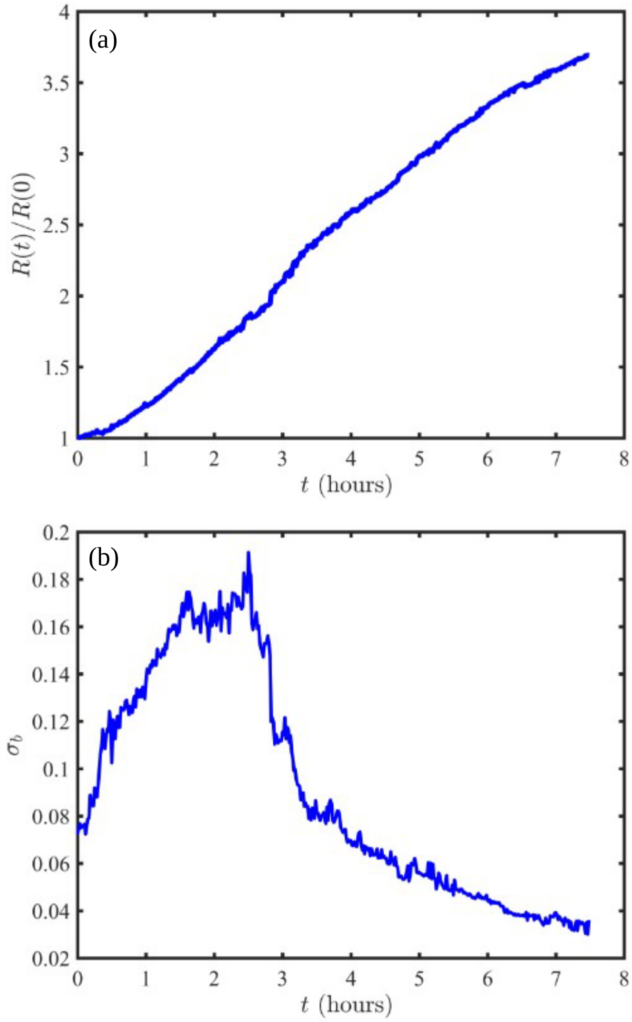

FIG. S1. Raw data showing for a particular experiment how the scaled biofilm radius $\mathcal{R}$ (a) and the relative deviation of the biofilm interface from a least-squares fitted circle σ_b (b) vary as functions of time.

biofilm growth timescale $\tau_0 = g^{-1}$ has to be determined. This was found through an iterative procedure, utilising all three experimental datasets to obtain a series of increasingly accurate estimates for g, $\{g_1, g_2, \cdots\}$, using the recursion relation that g_{n+1} is the g that minimises

$$\sum_i \left\{ \underset{j}{\text{avg}} \left([\mathcal{R}_e(t_j) - \mathcal{R}_{\Xi_i}(gt_j)]^2 \right) \right\}_i , \tag{S2}$$

where i iterates over all datasets and j over all points within the experimental dataset $\mathcal{R}_e(t_j) = R_e(t_j)/R_e(0)$ enumerated by i. $\mathcal{R}_{\tilde{\Xi}}(\tilde{\tau})$ is the solution to (S63) that is numerically computed for $\tau = \tilde{\tau}$ and $\Xi = \tilde{\Xi}$. Ξ_i is the value of Ξ that for the data set enumerated by i minimises the objective function

$$\underset{j}{\text{avg}} \left([\mathcal{R}_e(t_j) - \mathcal{R}_{\Xi}(g_n t_j)]^2 \right). \tag{S3}$$

Here, all minimizations were performed using the MATLAB inbuilt function fminbnd [S6]. This resulted in fitted values for the biofilm growth time scale of $g = 0.8574$ and for Ξ of 1.7352, 1.6702 and 1.3358 for the three different experiments.

FULL POROELASTIC FRAMEWORK

Below, we denote the region which the biofilm occupies ($r \leq R$) the inner region and the region outside of the biofilm ($r \geq R$) the outer region.

Inner Dimensional Vertical Boundary Conditions

Since horizontal motion of the upper PDMS sheet can be neglected, imposing no-slip boundary conditions at both the lower and upper boundaries yields

$$w_f = w_s = u_s = \zeta = \xi = 0 \text{ at } z = 0, \tag{S4a}$$

$$u_s = u_f = 0\,,\; w_f = w_s = \frac{\partial H}{\partial t} \text{ at } z = H. \tag{S4b}$$

Vertically integrating (3a) using these boundary conditions and (1) gives the continuity equation for vertically averaged biomass

$$\frac{\partial}{\partial t}\left(h\langle\phi\rangle\right) + \frac{1}{r}\frac{\partial}{\partial r}\left(rh\langle\phi\rangle\langle u_s\rangle\right) = gh\langle\phi\rangle. \tag{S5}$$

Applying global biomass conservation, the biomass volume $V = 2\pi\int_0^R rh\langle\phi\rangle dr$ satisfies $\partial V/\partial t = gV$. Expanding this out using the continuity equation (S5), (1) and the boundary conditions in (S4) gives

$$\frac{\partial R}{\partial t} = \frac{\langle\phi u_s\rangle}{\langle\phi\rangle}\Big|_R = \langle u_s\rangle\Big|_R. \tag{S6}$$

Modelling the upper sheet as a thin elastic beam, the pressure difference across the sheet is

$$[\Delta\tilde{p}]_-^+ = B\nabla^4 h - \gamma\nabla^2 h. \tag{S7}$$

Balancing normal stress at the interface between the biofilm and the sheet yields

$$B\nabla^4 h - \gamma\nabla^2 h = \tilde{p}\big|_h - (K + 4G/3)\frac{\partial\zeta}{\partial z}\Big|_h - (K - 2G/3)\frac{1}{r}\frac{\partial}{\partial r}(r\xi)\Big|_h \implies$$

$$p\big|_h = B\nabla^4 h - \gamma\nabla^2 h + (K + 4G/3)\frac{\partial\zeta}{\partial z}\Big|_h + \frac{K - 2G/3}{r}\frac{\partial}{\partial r}(r\xi)\Big|_h - \frac{\Pi_{\text{os}}\phi^3}{(1-\phi)^3}\Big|_h, \tag{S8}$$

where $\Pi_{\text{os}} = k_B T\beta^3/3\nu_0$.

Dimensionless shallow-layer scalings

We scale radial and vertical lengths with the initial radius $R_0 = R(t=0)$ and height $H_0 = h(r=0, t=0)$ of the biofilm respectively i.e $\{r,\, R\} \sim R_0$ and $\{z,\, h\} \sim H_0$. Since the characteristic time scale for the system is that for biofilm growth, we scale $t \sim 1/g$. Utilizing 3) and (S6), we find $\{u_f,\, u_s\} \sim U_s = gR_0$ and $\{w_f,\, w_s\} \sim gH_0$. Since $\boldsymbol{u_s}$ is defined as the material derivative of $\boldsymbol{\xi}$, we have $\xi \sim R_0$ and $\zeta \sim H_0$. By definition $\kappa \sim \kappa_0$. Finally, a leading order contribution to the pressure comes from the vertical confinement, i.e. (S8) implies $p \sim P_0 = BH_0/R_0^4$. We denote the dimensionless form of a function f by f^* and set for clarity

$$\rho = r^* = \frac{r}{R(0)},\ \mathcal{H} = h^* = \frac{h(r,t)}{h(0,0)},$$

$$\tau = \tau^* = gt,\ \mathcal{R} = R^* = \frac{R(t)}{R(0)},\ \mathcal{P} = p^* = \frac{p}{P_0}.$$

Inner Governing Equations

Using these scalings and setting $\epsilon = H_0/R_0$, the system of equations (3)-(9) becomes

$$\frac{\partial \phi}{\partial \tau} + \frac{\partial}{\partial z^*}\left(\phi w_s^*\right) + \frac{1}{\rho}\frac{\partial}{\partial \rho}\left(\rho \phi u_s^*\right) = \phi, \tag{S9a}$$

$$-\frac{\partial \phi}{\partial t} + \frac{\partial}{\partial z^*}\left((1-\phi) w_f^*\right) + \frac{1}{\rho}\frac{\partial}{\partial \rho}\left(\rho (1-\phi) u_f^*\right) = -\phi, \tag{S9b}$$

$$u_s = \frac{\rho}{\mathcal{R}}\frac{\partial \mathcal{R}}{\partial \tau}\frac{6z^*(\mathcal{H}-z^*)}{\mathcal{H}^2}, \tag{S9c}$$

$$W_1\left(w_f^* - w_s^*\right) = -\frac{\kappa^*}{(1-\phi)}\frac{\partial \mathcal{P}}{\partial z^*}, \tag{S9d}$$

$$\frac{\partial \mathcal{P}}{\partial \rho} = \chi \frac{\partial^2 \xi^*}{\partial {z^*}^2} + \mathcal{O}\left(\chi \epsilon^2\right), \tag{S9e}$$

$$\left(\frac{1}{W_1}\frac{\partial \mathcal{P}}{\partial z^*}\right) = P_1\left(\frac{\partial^2 \zeta^*}{\partial {z^*}^2} + \frac{\tilde{K}}{\rho}\frac{\partial}{\partial \rho}\left(\rho \frac{\partial \xi^*}{\partial z^*}\right) + \mathcal{O}\left(\epsilon^2\right)\right), \tag{S9f}$$

together with the continuity equation for vertically averaged biomass

$$\frac{\partial}{\partial \tau}\left(\mathcal{H}\varphi\right) + \frac{1}{\rho}\frac{\partial}{\partial \rho}\left(\rho \mathcal{H}\varphi v_s\right) = \mathcal{H}\varphi, \tag{S10}$$

and corresponding vertical boundary conditions

$$w_f^* = w_s^* = u_s^* = \zeta^* = \xi^* = 0 \text{ at } z^* = 0, \tag{S11a}$$

$$u_s^* = u_f^* = 0\,,\ w_f^* = w_s^* = \frac{\partial \mathcal{H}}{\partial t} \text{ at } z^* = \mathcal{H}. \tag{S11b}$$

$$\mathcal{P}\big|_{z^*=\mathcal{H}} = \nabla^4 \mathcal{H} - \gamma^* \nabla^2 \mathcal{H} - \Pi_{\text{os}}^* \frac{\phi^3}{(1-\phi)^3}\bigg|_{\mathcal{H}} + P_s\left(\frac{\partial \zeta^*}{\partial z^*}\bigg|_{\mathcal{H}} + \frac{1}{\rho}\left(\frac{K-2G/3}{K+4G/3}\right)\frac{\partial}{\partial \rho}\left(\rho \xi^*\right)\bigg|_{\mathcal{H}}\right), \tag{S11c}$$

where $\boldsymbol{u_s^*} = (u_s,\, w_s)$ can be expressed as the material derivative of $\boldsymbol{\xi^*} = (\xi,\, \zeta)$ using

$$w_s^* = \frac{\partial \zeta}{\partial \tau} + w_s^*\frac{\partial \zeta^*}{\partial z^*} + u_s^*\frac{\partial \zeta^*}{\partial \rho}, \tag{S12a}$$

$$u_s^* = \frac{\partial \xi^*}{\partial \tau} + w_s^*\frac{\partial \xi^*}{\partial z^*} + u_s^*\frac{\partial \xi^*}{\partial \rho}, \tag{S12b}$$

while $\{\tilde{K},\, W_1,\, \chi,\, P_1,\, \Pi_{\text{os}}^*,\, \gamma^*,\, P_s\}$ are non-dimensional constants that satisfy

$$\tilde{K} = \frac{K+G/3}{K+4G/3}, \quad W_1 = \frac{\mu_f g H_0^2}{\kappa_0 P_0}, \quad \chi = \frac{G}{\epsilon^2 P_0}, \tag{S13a}$$

$$P_1 = \frac{\kappa_0\left(K+4G/3\right)}{\mu_f g H_0^2},\ \Pi_{\text{os}}^* = \frac{R_0^4\, \Pi_{\text{os}}}{BH_0}, \tag{S13b}$$

$$\gamma^* = \frac{\gamma R_0^2}{B},\ P_s = \frac{R_0^4\left(K+4G/3\right)}{BH_0}. \tag{S13c}$$

Here, $\{W_1,\, \chi,\, P_1\}$ are dimensionless measures of the ability of flow to generate a vertical pressure gradient and the relative strength of the pressure gradients compared to elastic stresses in the horizontal and vertical respectively. γ^* and Π_{os}^* are the non-dimensional surface tension and osmotic pressure scaling groups. Finally, P_s measures the relative strength of the elastic stresses from the biofilm and the PDMS sheet at the upper interface.

Order of Magnitude Estimates for Parameters

In a typical experiment, the biofilm initially has height $H_0 \sim 10^{-5}$m and radius $R_0 \sim 10^{-4}$m. We assume that the dynamic viscosity of the nutrient rich liquid phase can be approximated by that of water, $\mu_f \sim 7.98 \times 10^{-4}$Pa s. From Seminara *et al.*, an order of magnitude estimate for the biofilm growth rate g is $g^{-1} \sim 2.3$ h [S1]. Furthermore, the characteristic biofilm permeability scale

$\kappa_0 \sim \xi_0^2$ where the biofilm mesh length scale $\xi_\infty \sim 50\,\mathrm{nm}$ i.e. $\kappa_0 \sim 2.5 \times 10^{-15}\mathrm{m}^2$

Picioreanu *et al.* estimated the mechanical properties of a range of different biofilms cultivated from activated sludge supernatant using optical coherence tomography, obtaining an effective Poisson ratio $\nu_b = 0.4$ and Young's modulus in the range $70-700\,\mathrm{Pa}$ [S7]. Assuming isotropy, we can thus estimate K and G as being in the range $K = E_b/3(1-2\nu_b) \sim 117 - 1170\,\mathrm{Pa}$ and $G = E_b/2(1+2\nu_b) \sim 19.4 - 194\,\mathrm{Pa}$ respectively.

The PDMS sheet has thickness $d \sim 10^{-4}\mathrm{m}$, Poisson's ratio $\nu \sim 0.5$ and Young's modulus $E \sim 1.9 \times 10^6\,\mathrm{Pa}$ (a value of 55 measured using a type A durometer). The matrix solid fraction β and the volume occupied by one monomer of extracellular matrix varies considerably, depending on a range of factors such as the species of bacteria and the nutrient concentration. Aiming to show that the osmotic pressure contribution can be neglected, we consider uppper and lower bounds for β and ν_0 respectively i.e. $\beta = \mathcal{O}(1)$ and $\nu_0 \sim 10^{-24}\mathrm{m}^3$. Finally, we estimate the surface tension between the biofilm and the sheet using that between water and PDMS ($\gamma \sim 4 \times 10^{-2}\mathrm{Nm}^{-2}$) [S8].

Hence, estimating values for the non-dimensional parameters $\{\epsilon,\, W_1,\, \chi,\, P_1,\, \gamma^*,\, \Pi^*_{\mathrm{os}},\, P_s,\, \epsilon_{\mathrm{outer}}\}$ gives

$$\epsilon = \frac{H_0}{R_0} \sim 10^{-1} \ll 1, \tag{S14a}$$

$$W_1 = \frac{12\mu_f g H_0 R_0 (1-\nu^2)}{\kappa_0 E} \sim 1.83 \times 10^{-7} \ll 1, \tag{S14b}$$

$$\chi = \frac{12G(1-\nu^2)}{\epsilon^3 E}\left(\frac{R_0}{d}\right)^3 \sim 9.19 \times \{10^{-2} - 10^{-1}\}, \tag{S14c}$$

$$P_1 = \frac{\kappa_0 (K + 4G/3)}{\mu_f g H_0^2} \sim 3.71 \times \{10^4 - 10^5\} \gg 1, \tag{S14d}$$

$$\gamma^* = \frac{12\gamma(1-\nu^2)}{Ed}\left(\frac{R_0}{d}\right)^2 \sim 2.25 \times 10^{-3} \ll 1, \tag{S14e}$$

$$\Pi_{\mathrm{os}} = \frac{4k_B T(1-\nu^2)\beta^3}{\epsilon \nu_0 E}\left(\frac{R_0}{d}\right)^3 \sim 6.60 \times 10^{-2} \ll 1, \tag{S14f}$$

$$P_s = \frac{12\left(1-\nu^2\right)(K+4G/3)}{\epsilon E}\left(\frac{R_0}{d}\right)^3 \sim 6.77 \times \{10^{-3} - 10^{-2}\} \ll 1, \tag{S14g}$$

$$\epsilon_{\mathrm{outer}} = \frac{144 g \mu_f \left(1-\nu^2\right)}{\epsilon^3 E}\left(\frac{R_0}{d}\right)^3 \sim 5.48 \times 10^{-9} \ll 1. \tag{S14h}$$

Stiff Elastic Confinement

Hence, under experimental conditions, we see that the upper elastic sheet is sufficiently stiff that $\{W_1,\, \gamma^*,\, \Pi^*_{\mathrm{os}},\, P_s\} \ll 1$ i.e. the dominant contribution to the pressure arises from the upper confinement. $P_1 \gg 1$ means that elastic stresses dominate the vertical pressure gradient. In general, $\chi = \mathcal{O}(1)$. Hence, the systems of governing equations given in ($S9$) – ($S11$) reduces to

$$\frac{\partial^2 \xi^*}{\partial z^{*2}} = \frac{1}{\chi}\frac{\partial \mathcal{P}}{\partial \rho}, \tag{S15a}$$

$$\frac{\partial^2 \zeta^*}{\partial z^{*2}} = -\frac{\tilde{K}}{\rho}\frac{\partial}{\partial \rho}\left(\rho \frac{\partial \xi^*}{\partial z^*}\right), \tag{S15b}$$

$$\frac{6\rho}{\mathcal{R}}\frac{\partial \mathcal{R}}{\partial \tau}\frac{z^*(\mathcal{H}-z^*)}{\mathcal{H}^2}\left(\left(1 - \frac{\partial \zeta^*}{\partial z^*}\right)\left(1 - \frac{\partial \xi^*}{\partial \rho}\right) - \frac{\partial \xi^*}{\partial z^*}\frac{\partial \zeta^*}{\partial \rho}\right) = \frac{\partial \xi^*}{\partial z^*}\frac{\partial \zeta^*}{\partial \tau} + \frac{\partial \xi^*}{\partial \tau}\left(1 - \frac{\partial \zeta^*}{\partial z^*}\right), \tag{S15c}$$

with corresponding boundary conditions

$$\left[\frac{\partial \xi^*}{\partial \tau}\right]_{z^*=0} = 0, \tag{S16a}$$

$$\left[\frac{\partial \xi^*}{\partial \tau} + \frac{\partial \mathcal{H}}{\partial \tau}\frac{\partial \xi^*}{\partial z^*}\right]_{z^*=\mathcal{H}} = 0, \tag{S16b}$$

$$\left[\frac{\partial \zeta^*}{\partial \tau}\right]_{z^*=0} = 0, \tag{S16c}$$

$$\left[\frac{\partial \zeta^*}{\partial \tau} + \frac{\partial \mathcal{H}}{\partial \tau}\frac{\partial \zeta^*}{\partial z^*}\right]_{z^*=\mathcal{H}} = \frac{\partial \mathcal{H}}{\partial \tau}. \tag{S16d}$$

where

$$\mathcal{P} = \nabla^4 \mathcal{H}. \tag{S17}$$

Since $\mathcal{P}$ is independent of z^*, integrating (S15a) twice with respect to z^* yields the functional form for ξ^*

$$\xi = b_0 + b_1 z^* + b_2 z^{*2}, \tag{S18}$$

where $\{b_i = b_i(\rho, \tau) : i \in [0,\, 1,\, 2]\}$ are independent of z^* and b_2 satisfies

$$b_2 = \frac{1}{2\chi}\frac{\partial \mathcal{P}}{\partial \rho} = \frac{1}{2\chi}\frac{\partial}{\partial \rho}\left(\nabla^4 \mathcal{H}\right). \tag{S19a}$$

(S16a) and (S16b) simplify respectively to give

$$\frac{\partial b_0}{\partial \tau} = 0 \Longrightarrow b_0 = b_0(\rho). \tag{S19b}$$

$$\frac{\partial}{\partial \tau}\left(\mathcal{H}b_1+\mathcal{H}^2 b_2\right)=0 \Longrightarrow b_1=\frac{B}{\mathcal{H}}-\mathcal{H}b_2, \tag{S19c}$$

where $B = B(\rho)$ is independent of τ and z^*. Hence, (S15b) becomes

$$\begin{aligned}\frac{\partial^2 \zeta^*}{\partial {z^*}^2} &= -\frac{\tilde{K}}{\rho}\frac{\partial}{\partial \rho}\left(\rho\frac{\partial \xi^*}{\partial z^*}\right)\\ &= -\frac{\tilde{K}}{\rho}\frac{\partial}{\partial \rho}\left(\frac{\rho B}{\mathcal{H}}+\rho b_2(2z^*-\mathcal{H})\right)\end{aligned} \tag{S20}$$

Integrating this twice with respect to z^* yields the functional form for ζ^*,

$$\zeta^* = a_0 + a_1 z^* + a_2 {z^*}^2 + a_3 {z^*}^3, \tag{S21}$$

where $\{a_i = a_i(\rho,\tau) : i \in [0,\ 1,\ 2,\ 3]\}$ are independent of z^* and a_2 and a_3 satisfy

$$a_2 = \frac{\tilde{K}}{2\rho}\frac{\partial}{\partial \rho}\left(\rho\mathcal{H}b_2 - \frac{\rho B}{\mathcal{H}}\right), \tag{S22a}$$

$$a_3 = -\frac{\tilde{K}}{3\rho}\frac{\partial}{\partial \rho}\left(\rho b_2\right). \tag{S22b}$$

(S16c) and (S16d) simplify respectively to give

$$\frac{\partial a_0}{\partial \tau} = 0 \Longrightarrow a_0 = a_0(\rho). \tag{S22c}$$

$$\frac{\partial}{\partial \tau}\left(\mathcal{H}a_1 + \mathcal{H}^2 a_2 + \mathcal{H}^3 a_3\right) = \frac{\partial \mathcal{H}}{\partial \tau} \Longrightarrow$$

$$a_1 = 1 + \frac{A}{\mathcal{H}} - \mathcal{H}a_2 - \mathcal{H}^2 a_3, \tag{S22d}$$

where $A = A(\rho)$ is independent of τ and z^*. Substituting (S18) and (S21) into (S15c) and equating the various powers of z^* gives the following set of six coupled equations for the variables a_j and b_k where $j \in [0,\ 1,\ 2,\ 3]$ and $k \in [0,\ 1,\ 2]$

$$\frac{\partial b_1}{\partial \tau} + b_1\frac{\partial a_1}{\partial \tau} - a_1\frac{\partial b_1}{\partial \tau} =$$

$$\frac{6\rho}{\mathcal{R}\mathcal{H}}\frac{\partial \mathcal{R}}{\partial \tau}\left((1-a_1)\left(1-\frac{\partial b_0}{\partial \rho}\right) - b_1\frac{\partial a_0}{\partial \rho}\right), \tag{S23a}$$

$$(1-a_1)\frac{\partial b_2}{\partial \tau} - 2a_2\frac{\partial b_1}{\partial \tau} + 2b_2\frac{\partial a_1}{\partial \tau} + b_1\frac{\partial a_2}{\partial \tau}$$

$$= -\frac{6\rho}{\mathcal{R}\mathcal{H}^2}\frac{\partial \mathcal{R}}{\partial \tau}\left((1-a_1)\left(1-\frac{\partial b_0}{\partial \rho}\right) - b_1\frac{\partial a_0}{\partial \rho}\right)$$

$$+\frac{6\rho}{\mathcal{R}\mathcal{H}}\frac{\partial \mathcal{R}}{\partial \tau}\Bigg(-2a_2\left(1-\frac{\partial b_0}{\partial \rho}\right) - \frac{\partial b_1}{\partial \rho}(1-a_1) - 2b_2\frac{\partial a_0}{\partial \rho} - b_1\frac{\partial a_1}{\partial \rho}\Bigg), \tag{S23b}$$

$$b_1\frac{\partial a_3}{\partial \tau} + 2b_2\frac{\partial a_2}{\partial \tau} - 2a_2\frac{\partial b_2}{\partial \tau} - 3a_3\frac{\partial b_1}{\partial \tau}$$

$$= -\frac{6\rho}{\mathcal{R}\mathcal{H}^2}\frac{\partial \mathcal{R}}{\partial \tau}\Bigg(-2a_2\left(1-\frac{\partial b_0}{\partial \rho}\right) - \frac{\partial b_1}{\partial \rho}(1-a_1) - 2b_2\frac{\partial a_0}{\partial \rho} - b_1\frac{\partial a_1}{\partial \rho}\Bigg)$$

$$+\frac{6\rho}{\mathcal{R}\mathcal{H}}\frac{\partial \mathcal{R}}{\partial \tau}\Bigg(-3a_3\left(1-\frac{\partial b_0}{\partial \rho}\right) + 2a_2\frac{\partial b_1}{\partial \rho} - (1-a_1)\frac{\partial b_2}{\partial \rho} - b_1\frac{\partial a_2}{\partial \rho} - 2b_2\frac{\partial a_1}{\partial \rho}\Bigg), \tag{S23c}$$

$$2b_2\frac{\partial a_3}{\partial \tau} - 3a_3\frac{\partial b_2}{\partial \tau}$$

$$= -\frac{6\rho}{\mathcal{R}\mathcal{H}^2}\frac{\partial \mathcal{R}}{\partial \tau}\Bigg(-3a_3\left(1-\frac{\partial b_0}{\partial \rho}\right) + 2a_2\frac{\partial b_1}{\partial \rho} - (1-a_1)\frac{\partial b_2}{\partial \rho} - b_1\frac{\partial a_2}{\partial \rho} - 2b_2\frac{\partial a_1}{\partial r}\Bigg), \tag{S23d}$$

$$2a_2\frac{\partial b_2}{\partial \rho} + 3a_3\frac{\partial b_1}{\partial \rho} - b_1\frac{\partial a_3}{\partial \rho} - 2b_2\frac{\partial a_2}{\partial \rho} = 0, \tag{S23e}$$

$$3a_3\frac{\partial b_2}{\partial \rho} - 2b_2\frac{\partial a_3}{\partial \rho} = 0. \tag{S23f}$$

In particular, equating co-efficients of ${z^*}^6$ gives

$$3a_3\frac{\partial b_2}{\partial \rho} = 2b_2\frac{\partial a_3}{\partial \rho}. \tag{S24}$$

We then have three possible cases:

1. Mode zero, $b_2 = 0 \Longrightarrow a_3 = 0$,
2. Mode one, $b_2 \neq 0$ but $a_3 = 0$,
3. Mode two, $b_2 \neq 0$ and $a_3 \neq 0$.

Mode zero

When $b_2 = 0$, $\mathcal{H}$ satisfies the differential equation

$$\frac{\partial \mathcal{P}}{\partial \rho} = 0 \frac{\partial}{\partial \rho}\left(\nabla^4 \mathcal{H}\right) = 0, \tag{S25}$$

which has the general solution

$$\mathcal{H} = A_{00} + A_{01}\,\rho^2 + A_{02}\,\rho^4 + A_{03}\,\log\rho + A_{04}\,\rho^2\log\rho. \tag{S26}$$

Note that this mode is dominant in the limit $\chi \ll 1$.

Mode one

When $a_3 = 0$, $\mathcal{H}$ satisfies the differential equation

$$\frac{\partial}{\partial \rho}(r b_2) = 0 \Longrightarrow b_2 = \frac{32}{\chi}\frac{A_{15}}{\rho} = \frac{1}{2\chi}\frac{\partial}{\partial\rho}\left(\nabla^4\mathcal{H}\right) \Longrightarrow$$

$$\frac{\partial}{\partial\rho}\left(\nabla^4\mathcal{H}\right) = \frac{64 A_{15}}{\rho}, \tag{S27}$$

which has the general solution

$$\mathcal{H} = A_{10} + A_{11}\,\rho^2 + A_{12}\,\rho^4 + A_{13}\,\log\rho + A_{14}\,\rho^2\log\rho + A_{15}\,\rho^4\log\rho. \tag{S28}$$

Mode two

When both b_2 and $a_3 \neq 0$, b_2 satisfies the differential equation

$$\frac{\partial}{\partial\rho}\left(\frac{b_2^3}{a_3^2}\right) = 0 \Longrightarrow b_2^3 = -\frac{9A_{25}}{2\chi\rho^2}\left(\frac{\partial}{\partial\rho}(\rho b_2)\right)^2. \tag{S29}$$

Employing the substitution $\tilde{b} = -\rho b_2$, this differential equation becomes separable and can be integrated to give

$$\int \tilde{b}^{3/2} d\tilde{b} = \int \sqrt{\frac{2\chi}{9\rho A_{25}}}\, d\rho \Longrightarrow \tag{S30}$$

$$\tilde{b} = \frac{9A_{25}}{2\chi\rho} \Longrightarrow b_2 = -\frac{9A_{25}}{2\chi\rho^2}. \tag{S31}$$

Hence, $\mathcal{H}$ satisfies the differential equation

$$\frac{\partial}{\partial\rho}\left(\nabla^4\mathcal{H}\right) = -\frac{9A_{25}}{\rho^2}, \tag{S32}$$

which has the general solution

$$\mathcal{H} = A_{20} + A_{21}\,\rho^2 + A_{22}\,\rho^4 + A_{23}\,\log\rho + A_{24}\,\rho^2\log\rho + A_{25}\,\rho^3. \tag{S33}$$

Horizontal Boundary Conditions

Define the inverse function of $\mathcal{R}(\tau)$, $\tau_1(\rho)$, as satisfying

$$\tau_1(\rho) = \begin{cases} \tau : \rho = \mathcal{R}(\tau) & \text{when } \rho > \mathcal{R}(0) = 1, \\ 0 & \text{otherwise.} \end{cases} \tag{S34}$$

Hence, constraining the pressure of the solid phase $(\sigma_l^*)_{z^*z^*}$ to be constant at the biofilm interface yields

$$\frac{\partial \zeta^*}{\partial z^*} + \frac{\tilde{K}}{\rho}\frac{\partial}{\partial\rho}(\rho\xi^*) = C_0 \Longrightarrow$$

$$(a_1 - 1) + \frac{\tilde{K}}{\rho}\frac{\partial}{\partial\rho}(\rho b_0) = C_0, \tag{S35}$$

at $\tau = \tau_1(\rho)$, where C_0 is a constant which is set from the initial pressure difference at $\tau = 0$ across the edge of the biofilm. From symmetry, $\mathcal{H}$ and $\mathcal{P}$ are even in ρ at $\rho = 0$, i.e.

$$\frac{\partial\mathcal{H}}{\partial\rho}(0,\tau) = \frac{\partial\mathcal{P}}{\partial\rho}(0,\tau) = 0. \tag{S36}$$

We assume that the biofilm grows uniformly at the interface, namely the vertically averaged biomass volume fraction φ satisfies

$$\varphi(\rho,\tau_1) = \varphi_\infty, \tag{S37a}$$

$$\frac{\partial\varphi}{\partial\tau}(\rho,\tau_1) = 0, \tag{S37b}$$

where φ_∞ is a constant.

Outer Governing equations

When $\rho > \mathcal{R}$, we have a lubrication flow of a single phase Newtonian fluid with viscosity μ_f. Hence, the vertically averaged fluid velocity $\langle u^* \rangle$ satisfies

$$\langle u^*\rangle = -\frac{\mathcal{H}^2}{\epsilon_{\text{outer}}}\frac{\partial}{\partial\rho}\left(B\nabla^4\mathcal{H}\right), \tag{S38}$$

leading to the continuity equation

$$\epsilon_{\text{outer}}\frac{\partial\mathcal{H}}{\partial t} = \frac{1}{\rho}\frac{\partial}{\partial\rho}\left(\rho\mathcal{H}^3\frac{\partial}{\partial\rho}(B\nabla^4\mathcal{H})\right), \tag{S39}$$

where the nondimensional constant ϵ_{outer} satisfies

$$\epsilon_{\text{outer}} = \frac{12 g \mu_f}{\epsilon^2 P_0}. \tag{S40}$$

From above, under experimental conditions, $\epsilon_{\text{outer}} \ll 1$. Hence, for $\rho \ll \epsilon_{\text{outer}}^{-1/6}$ and $\{\tau, \mathcal{H}\} = \mathcal{O}(1)$, (S39) becomes

$$\frac{1}{\rho}\frac{\partial}{\partial\rho}\left(\rho\mathcal{H}^3\frac{\partial}{\partial\rho}(B\nabla^4\mathcal{H})\right) = 0. \tag{S41}$$

Outer Boundary Conditions

In practice, the PDMS sheet has a finite radial extent at $\rho = \mathcal{R}_{\text{outer}} = R_{\text{outer}}/R(0)$ where $1 \ll \mathcal{R}_{\text{outer}} \ll \epsilon_{\text{outer}}^{-1/6}$. There are two possible kinds of boundary conditions that could be imposed here. If the sheet is clamped, namely fixed height and zero first derivative of height, we have

$$\mathcal{H}\left(\mathcal{R}_{\text{outer}}, \tau\right) = \mathcal{H}_{\infty}, \tag{S42a}$$

$$\frac{\partial \mathcal{H}}{\partial \rho}\left(\mathcal{R}_{\text{outer}}, \tau\right) = 0, \tag{S42b}$$

where $\mathcal{H}_{\infty} = h_{\infty}/H_0$ is a constant. Alternatively, if the sheet is not clamped, we impose free-beam conditions at $\rho = \mathcal{R}_{\text{outer}}$, namely

$$\frac{\partial^2 \mathcal{H}}{\partial \rho^2}\left(\mathcal{R}_{\text{outer}}, \tau\right) = 0. \tag{S43a}$$

$$\frac{\partial^3 \mathcal{H}}{\partial \rho^3}\left(\mathcal{R}_{\text{outer}}, \tau\right) = 0. \tag{S43b}$$

Interface Matching Conditions

A fluid flux balance at the biofilm edge yields

$$\left(\langle(1-\phi)u_f^*\rangle + \varphi\frac{\partial \mathcal{R}}{\partial \tau}\right)\bigg|_{\rho=\mathcal{R}^-} = \langle u^*\rangle\Big|_{\rho=\mathcal{R}^+}. \tag{S44}$$

At leading order in ϵ_{outer}, this simplifies to

$$\frac{\partial}{\partial \rho}\left(\nabla^4 \mathcal{H}\right)\bigg|_{\rho=\mathcal{R}^+} = 0. \tag{S45}$$

This requires that across $\rho = \mathcal{R}$, fourth and lower derivatives of $\mathcal{H}$ are continuous.

SIMPLIFICATION FROM A TWO TO A ONE PHASE SYSTEM

In the above, we have written down a set of governing equations for the full two-phase system, considering both the inner and the outer regions, with corresponding boundary conditions at $\rho = 0, \mathcal{R}$ and $\mathcal{R}_{\text{outer}}$. Working in the limit that $\mathcal{R}_{\text{outer}} \gg 1$, here we simplify our framework to just considering a single phase system, namely the inner region, together with boundary conditions at $\rho = 0$ and $\mathcal{R}$. Utilising the general form of the solution for $\mathcal{H}$ in the outer region, we achieve this by re-writing the far field boundary conditions at $\rho = \mathcal{R}_{\text{outer}}$ (expressed in terms of derivatives of $\mathcal{H}$ at $\rho = \mathcal{R}_{\text{outer}}$) in terms of derivatives of $\mathcal{H}$ at $\rho = \mathcal{R}$, noting that these derivatives are continuous across the biofilm interface.

Matching Machinery

Integrating (S41), using the boundary condition given in (S45), the general solution for $\mathcal{H}$ in the outer region is

$$\mathcal{H} = A_0 + A_1\rho^2 + A_2\rho^4 + A_3\log\rho + A_4\rho^2\log\rho. \tag{S46}$$

Defining vectors containing the constants of integration, the derivatives of $\mathcal{H}$ at the interface and the derivatives of $\mathcal{H}$ at the radial extent of the sheet, $\boldsymbol{A}_{\text{outer}}$, $\boldsymbol{\mathcal{H}}_{\text{interface}}$ and $\boldsymbol{\mathcal{H}}_{\text{outer}}$ respectively, as satisfying

$$\boldsymbol{A}_{\text{outer}} = [A_0,\, A_1,\, A_2,\, A_3,\, A_4]^T, \tag{S47a}$$

$$\begin{aligned}\boldsymbol{\mathcal{H}}_{\text{interface}} &= [\mathcal{H}_0,\, \mathcal{H}_1,\, \mathcal{H}_2,\, \mathcal{H}_3,\, \mathcal{H}_4]^T \\ &= \Big[\mathcal{H}(\mathcal{R},\tau),\, \frac{\partial \mathcal{H}}{\partial \rho}(\mathcal{R},\tau),\, \frac{\partial^2 \mathcal{H}}{\partial \rho^2}(\mathcal{R},\tau), \\ &\qquad \frac{\partial^3 \mathcal{H}}{\partial \rho^3}(\mathcal{R},\tau),\, \frac{\partial^4 \mathcal{H}}{\partial \rho^4}(\mathcal{R},\tau)\Big]^T,\end{aligned} \tag{S47b}$$

$$\begin{aligned}\boldsymbol{\mathcal{H}}_{\text{outer}} = \Big[&\mathcal{H}(\mathcal{R}_{\text{outer}},\tau),\, \frac{\partial \mathcal{H}}{\partial \rho}(\mathcal{R}_{\text{outer}},\tau),\, \frac{\partial^2 \mathcal{H}}{\partial \rho^2}(\mathcal{R}_{\text{outer}},\tau), \\ &\frac{\partial^3 \mathcal{H}}{\partial \rho^3}(\mathcal{R}_{\text{outer}},\tau),\, \frac{\partial^4 \mathcal{H}}{\partial \rho^4}(\mathcal{R}_{\text{outer}},\tau)\Big]^T,\end{aligned} \tag{S47c}$$

we can express $\boldsymbol{\mathcal{H}}_{\text{outer}}$ in terms of $\boldsymbol{\mathcal{H}}_{\text{interface}}$ using (S46):

$$\boldsymbol{H}_{\text{interface}} = \boldsymbol{\mathcal{M}}(\mathcal{R})\boldsymbol{A} \implies$$

$$\boldsymbol{A} = [\boldsymbol{\mathcal{M}}(\mathcal{R})]^{-1}\boldsymbol{H}_{\text{interface}} \implies$$

$$\boldsymbol{\mathcal{H}}_{\text{outer}} = \boldsymbol{\mathcal{M}}(\mathcal{R}_{\text{outer}})[\boldsymbol{\mathcal{M}}(\mathcal{R})]^{-1}\boldsymbol{H}_{\text{interface}}, \tag{S48}$$

where

$$\boldsymbol{M_1}(x) = \begin{pmatrix} 1 & x^2 & x^4 & \log x & x^2\log x \\ 0 & 2x & 4x^3 & 1/x & x + 2x\log x \\ 0 & 2 & 12x^2 & -1/x^2 & 2\log x + 3 \\ 0 & 0 & 24x & 2/x^3 & 2/x \\ 0 & 0 & 24 & -6/x^4 & -2/x^2 \end{pmatrix}. \tag{S49}$$

Re-writing the Far-field Clamped Boundary Conditions

Using (S48), the boundary conditions at $\rho = \mathcal{R}_{outer}$ given in (S42) can be written in the form

$$\begin{aligned}&\frac{\mathcal{R}_{outer}^4}{64}\left(\mathcal{H}_4 + \frac{2\mathcal{H}_3}{\mathcal{R}} - \frac{\mathcal{H}_2}{\mathcal{R}^2} + \frac{\mathcal{H}_1}{\mathcal{R}^3}\right) \\ &- \frac{\mathcal{R}^2\mathcal{R}_{\text{outer}}^2}{8}\log\left(\frac{\mathcal{R}_{\text{outer}}}{\mathcal{R}}\right)\left(\mathcal{H}_4 - \frac{3\mathcal{H}_2}{\mathcal{R}^2} + \frac{3\mathcal{H}_1}{\mathcal{R}^3}\right) \\ &= \mathcal{O}\left(\mathcal{H}_0\left(\frac{\mathcal{R}_{\text{outer}}}{\mathcal{R}}\right)^2\right),\end{aligned} \tag{S50a}$$

and

$$-\frac{\mathcal{R}^2\mathcal{R}_{\text{outer}}^2}{8}\log\left(\frac{\mathcal{R}_{\text{outer}}}{\mathcal{R}}\right)\left(\mathcal{H}_4-\frac{3\mathcal{H}_2}{\mathcal{R}^2}+\frac{3\mathcal{H}_1}{\mathcal{R}^3}\right)$$
$$=\mathcal{O}\left(\mathcal{H}_0\left(\frac{\mathcal{R}_{\text{outer}}}{\mathcal{R}}\right)^2\right). \quad \text{(S50b)}$$

These two conditions rearrange to give

$$\mathcal{H}_4-\frac{3\mathcal{H}_2}{\mathcal{R}^2}+\frac{3\mathcal{H}_1}{\mathcal{R}^3}=\mathcal{O}\left(\frac{\mathcal{H}_0}{\mathcal{R}^4\log\left(\mathcal{R}_{\text{outer}}/\mathcal{R}\right)}\right), \quad \text{(S50c)}$$

$$\mathcal{H}_4+\frac{2\mathcal{H}_3}{\mathcal{R}}-\frac{\mathcal{H}_2}{\mathcal{R}^2}+\frac{\mathcal{H}_1}{\mathcal{R}^3}=\mathcal{O}\left(\frac{\mathcal{H}_0}{\mathcal{R}^2\mathcal{R}_{\text{outer}}^2}\right). \quad \text{(S50d)}$$

Moving back to tensorial notation, we see that to leading order in $\mathcal{R}_{\text{outer}}$ the far field boundary conditions can be rewritten as the zero pressure condition

$$\nabla^4\mathcal{H}(\mathcal{R},\tau)=0+\mathcal{O}\left(\frac{\mathcal{H}_0}{\mathcal{R}^2\mathcal{R}_{\text{outer}}^2}\right), \quad \text{(S50e)}$$

together with the force free condition

$$\frac{\partial}{\partial\rho}\left(\nabla^2\mathcal{H}(\mathcal{R},\tau)\right)=0+\mathcal{O}\left(\frac{\mathcal{H}_0}{\mathcal{R}^4\log\left(\mathcal{R}_{\text{outer}}/\mathcal{R}\right)}\right). \quad \text{(S50f)}$$

Re-writing the Far-field Free Beam Boundary Conditions

In the same way, using (S48), the boundary conditions at $\rho=\mathcal{R}_{outer}$ given in (S43) can be written in the form

$$\frac{3\mathcal{R}_{outer}^4}{16}\left(\mathcal{H}_4+\frac{2\mathcal{H}_3}{\mathcal{R}}-\frac{\mathcal{H}_2}{\mathcal{R}^2}+\frac{\mathcal{H}_1}{\mathcal{R}^3}\right)$$
$$-\frac{\mathcal{R}^2\mathcal{R}_{\text{outer}}^2}{4}\log\left(\frac{\mathcal{R}_{\text{outer}}}{\mathcal{R}}\right)\left(\mathcal{H}_4-\frac{3\mathcal{H}_2}{\mathcal{R}^2}+\frac{3\mathcal{H}_1}{\mathcal{R}^3}\right)$$
$$=\mathcal{O}\left(\mathcal{H}_0\left(\frac{\mathcal{R}_{\text{outer}}}{\mathcal{R}}\right)^2\right), \quad \text{(S51a)}$$

and

$$-4\mathcal{R}^2\mathcal{R}_{\text{outer}}^2\log\left(\frac{\mathcal{R}_{\text{outer}}}{\mathcal{R}}\right)\left(\mathcal{H}_4-\frac{3\mathcal{H}_2}{\mathcal{R}^2}+\frac{3\mathcal{H}_1}{\mathcal{R}^3}\right)$$
$$=\mathcal{O}\left(\mathcal{H}_0\left(\frac{\mathcal{R}_{\text{outer}}}{\mathcal{R}}\right)^2\right). \quad \text{(S51b)}$$

These two conditions rearrange to give

$$\mathcal{H}_4-\frac{3\mathcal{H}_2}{\mathcal{R}^2}+\frac{3\mathcal{H}_1}{\mathcal{R}^3}=\mathcal{O}\left(\frac{\mathcal{H}_0}{\mathcal{R}^4\log\left(\mathcal{R}_{\text{outer}}/\mathcal{R}\right)}\right), \quad \text{(S51c)}$$

$$\mathcal{H}_4+\frac{2\mathcal{H}_3}{\mathcal{R}}-\frac{\mathcal{H}_2}{\mathcal{R}^2}+\frac{\mathcal{H}_1}{\mathcal{R}^3}=\mathcal{O}\left(\frac{\mathcal{H}_0}{\mathcal{R}^2\mathcal{R}_{\text{outer}}^2}\right). \quad \text{(S51d)}$$

Moving back to tensorial notation, we see that to leading order in $\mathcal{R}_{\text{outer}}$ the far field boundary conditions can be rewritten as the zero pressure condition

$$\nabla^4\mathcal{H}(\mathcal{R},\tau)=0+\mathcal{O}\left(\frac{\mathcal{H}_0}{\mathcal{R}^2\mathcal{R}_{\text{outer}}^2}\right), \quad \text{(S51e)}$$

together with the force free condition

$$\frac{\partial}{\partial\rho}\left(\nabla^2\mathcal{H}(\mathcal{R},\tau)\right)=0+\mathcal{O}\left(\frac{\mathcal{H}_0}{\mathcal{R}^4\log\left(\mathcal{R}_{\text{outer}}/\mathcal{R}\right)}\right). \quad \text{(S51f)}$$

Noting that (S50e), (S50f) and (S51e), (S51f) are identical, we see that both set of boundary conditions at $\rho=\mathcal{R}_{\text{outer}}$, when rewritten in terms of derivatives of $\mathcal{H}$ at $\rho=\mathcal{R}$, give at leading order in $\mathcal{R}_{\text{outer}}$ the same conditions for $\mathcal{H}$.

MODE ZERO SIMILARITY SOLUTION

To make further analytic progress, we look for a similarity solution in the mode zero case i.e.

$$b_2=0\Longrightarrow\frac{\partial}{\partial\rho}\left(\nabla^4\mathcal{H}\right)=0\Longrightarrow$$

$$\mathcal{H}=F\left(A-\left(\frac{\rho}{\mathcal{R}}\right)^2\right), \quad \text{(S52)}$$

where we have utilised the horizontal boundary conditions for $\mathcal{H}$, A is a constant and $F=F(\tau)$ is independent of ρ. Evaluating (S10) at $\rho=\mathcal{R}$ then gives

$$\frac{\partial\mathcal{H}}{\partial\tau}(\mathcal{R},\tau)+\frac{1}{\mathcal{R}}\frac{\partial}{\partial\rho}\left(\rho\mathcal{H}v_s\right)\Big|_{\mathcal{R}}=\mathcal{H}(\mathcal{R},\tau)\Longrightarrow$$

$$(A-1)\left[\frac{\partial F}{\partial\tau}+\frac{2F}{\mathcal{R}}\frac{\partial\mathcal{R}}{\partial\tau}-F\right]=0\Longrightarrow F=\frac{F_0e^\tau}{\mathcal{R}^2}. \quad \text{(S53)}$$

Applying the initial condition $\mathcal{H}_0(\rho=0,\tau=0)=1$ and defining the incline ratio m_0, a measure of the initial flatness of the biofilm, as satisfying

$$m_0=\frac{h(r=R(0),t=0)}{h(r=0,t=0)}=\mathcal{H}(\rho=1,\tau=0), \quad \text{(S54)}$$

we find $F_0=1-m_0$ and $A=1/(1-m_0)$ i.e.

$$\mathcal{H}=\frac{e^\tau}{\mathcal{R}^2}\left(1-(1-m_0)\left(\frac{\rho}{\mathcal{R}}\right)^2\right). \quad \text{(S55)}$$

Defining $f=f(\rho,\tau)=\mathcal{H}\varphi e^\tau$, the continuity equation (S10) becomes

$$\frac{\partial f}{\partial\tau}=-\left(\frac{1}{\mathcal{R}}\frac{\partial\mathcal{R}}{\partial\tau}\right)\frac{1}{\rho}\frac{\partial}{\partial\rho}\left(\rho^2f\right). \quad \text{(S56)}$$

Looking for a similarity solution of the form $f = f_1(\mathcal{R})f_2(\eta)$ where $\eta = \rho/\mathcal{R}$, this simplifies to give

$$\frac{\partial f_1}{\partial \mathcal{R}} = -\frac{2f_1}{\mathcal{R}} \implies f_1 = \frac{1}{\mathcal{R}^2} \implies \varphi = \varphi_0(\eta), \tag{S57}$$

Here $\varphi_0(\rho) = \varphi(\rho, \tau = 0)$ is set from the initial conditions (from § φ_0 must satisfy the properties $\varphi = \phi_\infty$ and $\partial\varphi/\partial\rho = 0$ at $\tau = 0$).

Finally, we seek an analytical solution for $\boldsymbol{\xi^*} = (\xi^*, \zeta^*)$ with minimal z^* dependence. Setting $a_2 = 0$, (S18) and (S21) simplify to become

$$\zeta^* = a_0 + z^*\left(1 + \frac{A}{\mathcal{H}}\right), \quad \xi^* = b_0 + \frac{Bz^*}{\mathcal{H}}, \tag{S58}$$

where $\{a_0, b_0, A, B\}$ are all independent of τ. (S15a) is automatically satisfied. (S15b) and (S15c) reduce to

$$\frac{\partial}{\partial\rho}\left(\frac{\rho B}{\mathcal{H}}\right) = 0 \implies \frac{\rho B(\rho)}{F(\tau)\left(A - (\rho/\mathcal{R})^2\right)} \implies B = 0. \tag{S59}$$

$$\frac{6\rho}{\mathcal{R}\mathcal{H}}\frac{\partial\mathcal{R}}{\partial\tau}\left(-\frac{A}{\mathcal{H}}\left(1 - \frac{\partial b_0}{\partial\rho}\right)\right) = 0 \implies \tag{S60}$$

$$\frac{\partial b_0}{\partial\rho} = 1 \implies b_0 = \xi_0 + \rho, \tag{S61}$$

where ξ_0 is a constant set from the initial conditions. Finally, we set for simplicity A to a constant ζ_0. Hence, the stress boundary condition (S35) simplifies to become

$$\frac{\zeta_0}{\mathcal{H}} + \frac{\tilde{K}}{\rho}\frac{\partial}{\partial\rho}\left(B_0\rho + \rho^2\right) = C_0 \text{ at } \rho = \mathcal{R}. \tag{S62}$$

Applying the initial condition $\mathcal{R}(0) = 1$, we recover the cubic equation which describes the evolution of $\mathcal{R}$

$$e^{-\tau}\mathcal{R}^3 + \mathcal{R}\left(\Xi - 1\right) - \Xi = 0, \tag{S63}$$

Here, the non-dimensional evolution constant Ξ is

$$\Xi = \frac{\tilde{K}\xi_0 m_0}{\zeta_0}, \tag{S64}$$

and is thus is determined from the initial conditions as the product of the incline ratio and a ratio between horizontal and vertical stresses.

Now, Cardano's formula for depressed cubic equations states that for the equation

$$x^3 + px + q = 0, \tag{S65}$$

where p and q are real, if $\Lambda(p, q) = 4p^3 + 27q^2 > 0$ then the equation has the single real root

$$x = \left(-\frac{q}{2} + \sqrt{\frac{q^2}{4} + \frac{p^3}{27}}\right)^{1/3} + \left(-\frac{q}{2} - \sqrt{\frac{q^2}{4} + \frac{p^3}{27}}\right)^{1/3}, \tag{S66}$$

with the other two roots being complex conjugates. If $\Lambda < 0$ there are three real roots but they can not be represented by an algebraic expression involving only real numbers. This was called by Cardano the *casus irreducibilis* (Latin for 'the irreducible case').

For (S63), we have

$$p = e^\tau(\Xi - 1), \tag{S67a}$$

$$q = -e^\tau\Xi, \tag{S67b}$$

$$\Lambda = e^{2\tau}\left(4e^\tau\left(\Xi - 1\right)^3 + 27\Xi^2\right). \tag{S67c}$$

Hence, $\Lambda < 0$ when $\Xi < 1$ and τ satisfies

$$\tau > \tau_{\text{crit}} = \log\left(\frac{27\Xi^2}{4(1 - \Xi)^3}\right). \tag{S68}$$

Thus, for general Ξ and τ, (S63) does not admit an analytical solution. Instead, this cubic equation is solved numerically using the MATLAB inbuilt function fzero [S6]. Since cubic equations have up to three real roots, we select the correct root by locating the root that is closest to the value for $\mathcal{R}$ found at the previous time step, noting that by definition $\mathcal{R}(\tau = 0) = 1$.

NEWTONIAN MODEL

Here, for comparison, we analyze the corresponding mathematical model in which, as in Seminara et. al. [S1], the intrinsic elasticity of the biofilm extracellular matrix is neglected. In this case, a solution with power law growth tending to a maximum finite biofilm radius is not supported, demonstrating that matrix elasticity is essential to capture the behavior we have observed experimentally.

Dimensionless shallow-layer scalings

In the same way as for the poroelastic model, we scale radial and vertical lengths with the initial radius $R_0 = R(t = 0)$ and height $H_0 = h(r = 0, t = 0)$ of the biofilm, respectively, permeability with the characteristic permeability scale κ_0, pressure with the vertical confinement pressure scale and time with thath for biofilm growth i.e. $\{r, R\} \sim R_0$, $\{z, h\} \sim H_0$, $\kappa \sim \kappa_0$, $p \sim P_0 = BH_0/R_0^4$ and $t \sim 1/g$. Hence, we find $\{u_f, u_s\} \sim gR_0$ and $\{w_f, w_s\} \sim gH_0$. Similarly, we denote the dimensionless form of a function f by f^* and set for clarity

$$\rho = r^* = \frac{r}{R(0)}, \ \mathcal{H} = h^* = \frac{h(r,t)}{h(0,0)}, \ \tau = \tau^* = gt,$$

$$\mathcal{R} = R^* = \frac{R(t)}{R(0)}, \ \mathcal{P} = p^* = \frac{p}{P_0}.$$

As above, we assume that the biomass volume fraction ϕ is independent of z^*,

$$\frac{\partial \phi}{\partial z^*} = 0. \tag{S69}$$

In nondimensional form, the governing equations for this system become

$$\frac{\partial \phi}{\partial \tau} + \frac{1}{\rho}\frac{\partial}{\partial \rho}(\rho \phi u_s^*) + \frac{\partial}{\partial z^*}(\phi w_s^*) = \phi, \tag{S70a}$$

$$-\frac{\partial \phi}{\partial \tau} + \frac{1}{\rho}\frac{\partial}{\partial \rho}(\rho(1-\phi) u_f^*) + \frac{\partial}{\partial z^*}((1-\phi) w_f^*) = -\phi, \tag{S70b}$$

$$u_s^* - u_f^* = \frac{\epsilon^2}{W_1}\frac{\kappa^*}{1-\phi}\frac{\partial \mathcal{P}}{\partial \rho}, \tag{S70c}$$

$$w_s^* - w_f^* = \frac{1}{W_1}\frac{\kappa^*}{1-\phi}\frac{\partial \mathcal{P}}{\partial z^*}, \tag{S70d}$$

$$\frac{\epsilon^2}{W_1}\frac{\partial \mathcal{P}}{\partial \rho} = \mu \left(\frac{\partial^2 u_s^*}{\partial z^{*2}} + \left(\frac{H_0}{R_0}\right)^2 \frac{1}{\rho}\frac{\partial}{\partial \rho}\left(\rho \frac{\partial u_s^*}{\partial \rho}\right)\right), \tag{S70e}$$

$$\frac{1}{W_1}\frac{\partial \mathcal{P}}{\partial z^*} = \mu \left(\frac{\partial^2 w_s^*}{\partial z^{*2}} + \left(\frac{H_0}{R_0}\right)^2 \frac{1}{\rho}\frac{\partial}{\partial \rho}\left(\rho \frac{\partial w_s^*}{\partial \rho}\right)\right), \tag{S70f}$$

where the non-dimensional constants $\{\mu, W_1\}$ satisfy

$$\mu = \frac{\kappa_0}{H_0^2}\frac{\mu_s}{\mu_f}, \quad W_1 = \frac{\mu_f g H_0^2}{\kappa_0 P_0}. \tag{S71}$$

Here W_1, defined in (S13), is a dimensionless measure of the ability of flow to generate a vertical pressure gradient, μ is the non-dimensional biofilm viscosity scaling group and μ_s is the dimensional Newtonian viscosity of the biofilm solid phase. Utilising the typical experimental values for the scalings given in appendix , together with $\mu_s \sim 10^2$ Pa s we see that $\{W_1, \epsilon^{-2} W_1\} \ll 1$ while $\mu \approx 2.8 = \mathcal{O}(1)$.

Vertical boundary conditions

As before, imposing no-slip boundary conditions at both the lower and upper boundaries gives

$$w_f^* = w_s^* = u_s^* \text{ at } z^* = 0, \tag{S72a}$$

$$u_s^* = u_f^* = 0\,,\; w_f^* = w_s^* = \frac{\partial \mathcal{H}}{\partial t} \text{ at } z^* = \mathcal{H}. \tag{S72b}$$

Balancing normal stress at the biofilm sheet interface gives

$$\mathcal{P}\Big|_{z^*=\mathcal{H}} = \mathcal{P}_0 + \nabla^4 \mathcal{H} + 2\mu W_1 \frac{\partial w_s^*}{\partial z^*}\Big|_{z^*=\mathcal{H}} \tag{S72c}$$

where $\mathcal{P}_0$ is a constant reference pressure. Working at leading order in W_1, combining (S70d) and (S72c) gives

$$\frac{\partial \mathcal{P}}{\partial z^*} = 0 + \mathcal{O}(W_1) \Longrightarrow \mathcal{P} = \mathcal{P}_0 + \nabla^4 \mathcal{H} + \mathcal{O}(W_1). \tag{S73a}$$

Hence, applying (S70c) gives the differential equation for $\mathcal{H}$

$$\frac{\partial}{\partial \rho}\left(\nabla^4 \mathcal{H}\right) = 0 + \mathcal{O}(\epsilon^{-2} W_1). \tag{S73b}$$

Similarly, combining ((S70d) and (S70f)) and ((S70d) and (S70f)) yields respectively

$$u_s^* - u_f^* = \mu \frac{\kappa^*}{1-\phi}\frac{\partial^2 u_s^*}{\partial z^{*2}} + \mathcal{O}\left(\epsilon^2\right), \tag{S73c}$$

$$w_s^* - w_f^* = \mu \frac{\kappa^*}{1-\phi}\frac{\partial^2 w_s^*}{\partial z^{*2}} + \mathcal{O}\left(\epsilon^2\right). \tag{S73d}$$

Finally, integrating (S70e) using the boundary conditions given in (S72a) and (S72b) gives

$$u_s^* = -\frac{z^*(\mathcal{H} - z^*)}{2\mu}\left(\frac{\epsilon^2}{W_1}\frac{\partial \mathcal{P}}{\partial \rho}\right) + \mathcal{O}(\epsilon^2). \tag{S73e}$$

Vertically averaged governing equations

We denote vertically averaged quantities by triangular brackets, namely for an arbitrary function f we define $\langle f \rangle = \mathcal{H}^{-1}\int_0^{\mathcal{H}} f\, dz^*$, and for clarity set

$$\varphi = \langle \phi \rangle,\; k = \langle \kappa \rangle,\; v_s = \langle u_s \rangle = -\frac{\mathcal{H}^2}{12\mu}\left(\frac{\epsilon^2}{W_1}\frac{\partial \mathcal{P}}{\partial \rho}\right) + \mathcal{O}(\epsilon^2).$$

Integrating (S70a) in the z^* direction yields

$$\frac{\partial}{\partial \tau}(\varphi \mathcal{H}) + \frac{1}{\rho}\frac{\partial}{\partial \rho}\left(\rho \langle \phi u_s^* \rangle \mathcal{H}\right) = \varphi \mathcal{H}. \tag{S74}$$

Similarly, integrating (S70a)+(S70b) in the z^* direction gives the continuity equation

$$\begin{aligned}\frac{\partial \mathcal{H}}{\partial \tau} &= \frac{1}{\rho}\frac{\partial}{\partial \rho}\left(\rho \mathcal{H}\left(\frac{k\epsilon^2}{W_1}\frac{\partial \mathcal{P}}{\partial \rho} - v_s\right)\right) \\ &= \frac{1}{\rho}\frac{\partial}{\partial \rho}\left(\rho \mathcal{H}\left(k + \frac{\mathcal{H}^2}{12\mu}\right)\left(\frac{\epsilon^2}{W_1}\frac{\partial}{\partial \rho}\left(\nabla^4 \mathcal{H}\right)\right)\right) \\ &+ \mathcal{O}(\epsilon^2)\end{aligned} \tag{S75}$$

Vertically averaged boundary conditions

As in the poroelastic model, we have the boundary conditions

$$\frac{\partial \mathcal{H}}{\partial \rho} = \frac{\partial \mathcal{P}}{\partial \rho} = 0 \text{ at } \rho = 0, \tag{S76a}$$

$$\nabla^4 \mathcal{H} = \mathcal{R}^3 \frac{\partial^3 \mathcal{H}}{\partial \rho^3} + \mathcal{R}\frac{\partial^2 \mathcal{H}}{\partial \rho^2} - \frac{\partial \mathcal{H}}{\partial \rho} = 0 \text{ at } \rho = \mathcal{R}, \tag{S76b}$$

$$\varphi = \varphi_\infty \text{ at } \rho = \mathcal{R}, \tag{S76c}$$

$$\frac{\partial \varphi}{\partial \tau} = 0 \text{ at } \rho = \mathcal{R}. \tag{S76d}$$

Similarly, polymer volume conservation yields the evolution condition

$$\frac{\partial \mathcal{R}}{\partial t} = \frac{\langle \phi\, u_s^* \rangle}{\phi_\infty} = v_s \text{ at } \rho = \mathcal{R}(t). \tag{S77}$$

As above, (S73b) together with the boundary conditions in (S76b) admits the similarity solution

$$\mathcal{H} = F_0 + F_1 \rho^2, \tag{S78}$$

where $F_0 = F_0(\tau)$ and $F_1 = F_1(\tau)$ are independent of ρ. Integrating (S75) with respect to ρ then gives

$$\frac{\rho^2}{2}\frac{\partial F_0}{\partial \tau} + \frac{\rho^4}{4}\frac{\partial F_1}{\partial \tau} = -\frac{12\rho\mu}{\mathcal{H}}\left(k + \frac{\mathcal{H}^2}{12\mu}\right) \Longrightarrow$$

$$v_s = -\frac{\mathcal{H}}{\rho\,(12\mu k + \mathcal{H}^2)}\left(\frac{\rho^2}{2}\frac{\partial F_0}{\partial \tau} + \frac{\rho^4}{4}\frac{\partial F_1}{\partial \tau}\right). \tag{S79}$$

Here, we have used (S76a) to set the integration constant to 0. In general, one can not make further analytic progress.

Finite radius solution

Experimentally, we see that the radius of the biofilm tends to a finite value i.e. the system supports a biofilm with constant radius $\mathcal{R} = \mathcal{R}_\infty$. In this case, (S77) simplifies to give

$$v_s\big|_{\mathcal{R}_\infty} = 0 \Longrightarrow \frac{\partial F_0}{\partial \tau} + \frac{\mathcal{R}_\infty^2}{2}\frac{\partial F_1}{\partial \tau} = 0 \Longrightarrow$$

$$F_0 = C_1 - \frac{\mathcal{R}_\infty^2 F_1}{2}, \tag{S80}$$

where C_1 is a constant. Since $\mathcal{H} > 0\, \forall \rho \in [0, \mathcal{R}_\infty]$, evaluating $\mathcal{H}$ at $\rho = 0$ and $\rho = \mathcal{R}_\infty$ gives

$$\mathcal{H} = C_1 + F_1\left(\rho^2 - \frac{\mathcal{R}_\infty^2}{2}\right) \Longrightarrow$$

$$\left\{ \mathcal{H}\big|_0 = C_1 - \frac{F_1 \mathcal{R}_\infty^2}{2},\ \mathcal{H}\big|_{\mathcal{R}_\infty} = C_1 + \frac{F_1 \mathcal{R}_\infty^2}{2} \right\}, \tag{S81}$$

namely C_1 is positive with the lower bound $C_1 > \mathcal{R}_\infty^2 |F_1|/2$. Similarly, differentiating (S79) with respect to ρ at $\rho = \mathcal{R}_\infty$ gives

$$\begin{aligned}\frac{\partial v_s}{\partial \rho}\Big|_{\mathcal{R}_\infty} &= -\frac{\mathcal{H}}{12\mu k + \mathcal{H}^2}\left(\frac{\partial F_0}{\partial \tau} + \rho^2 \frac{\partial F_1}{\partial \tau}\right) \\ &= -\frac{\mathcal{H}\mathcal{R}_\infty^2}{2\,(\mathcal{H}^2 + 12\mu k)}\frac{\partial F_1}{\partial \tau}.\end{aligned} \tag{S82}$$

Hence, evaluating (S74) at $\rho = \mathcal{R}$, utilising the boundary conditions given above gives

$$\frac{\partial \mathcal{H}}{\partial \tau}\Big|_{\mathcal{R}_\infty} + \left(\mathcal{H}\frac{\partial v_s}{\partial \rho}\right)\Big|_{\mathcal{R}_\infty} = \mathcal{H}\big|_{\mathcal{R}_\infty} \Longrightarrow$$

$$C_2 \frac{\partial F_1}{\partial \tau} = (F_1 + C_3)\left(C_2 + (F_1 + C_3)^2\right) \Longrightarrow$$

$$\begin{aligned}\tau &= \int \frac{C_2}{(F_1 + C_3)\,(C_2 + (F_1 + C_3)^2)}\, dF_1 \\ &= \int \frac{1}{F_1 + C_3} - \frac{(F_1 + C_3)}{C_2 + (F_1 + C_3)^2}\, dF_1 \\ &= \ln(F_1 + C_3) - \frac{1}{2}\ln\left(C_2 + (F_1 + C_3)^2\right) - \frac{1}{2}\ln(\tilde{C}) \\ &= \frac{1}{2}\ln\left(\frac{(F_1 + C_3)^2}{\tilde{C}\,(C_2 + (F_1 + C_3)^2)}\right) \Longrightarrow\end{aligned}$$

$$(F_1 + C_3)^2 = \frac{\tilde{C} C_2 e^{2\tau}}{1 - \tilde{C} e^{2\tau}}, \tag{S83}$$

where $\tilde{C}$ is a constant of integration and the positive constants C_2 and C_3 satisfy

$$C_2 = \frac{48\mu}{\mathcal{R}_\infty^4} k(\varphi_\infty), \quad C_3 = \frac{2C_1}{\mathcal{R}_\infty^2}. \tag{S84}$$

Since the right hand side of (S83) is non-negative for all τ, $\tilde{C} = 0$ and thus $F_1 = -C_3$. However, this then gives $\mathcal{H} = 0$ at $\rho = \mathcal{R}_\infty$ which is a contradiction. Hence, the Newtonian model does not support a constant radius solution and thus does not agree with experiments.

[S1] A. Seminara, T.E. Angelini. J.N. Wilking, H. Vlamakis, S. Ebrahim, R. Kolter, D.A. Weitz, and M. P. Brenner, Osmotic spreading of *Bacillus subtilis* biofilms driven by an extracellular matrix, Proc. Natl. Acad. Sci. USA **109**, 1116 (2012).

[S2] R. Martinez-Corral, J. Liu, A. Prindle, G. M. Süel, and J. Garcia-Ojalvo, Metabolic basis of brain-like electrical signalling in bacterial communities, Phil. Trans. R. Soc. B **374**, 20180382 (2019).

[S3] J. Liu, A. Prindle, J. Humphries, M. Gabalda-Sagarra, D.D. Lee, S. Ly, J. Garcia-Ojalvo, and G. M. Süel, Metabolic co-dependence gives rise to collective oscillations within biofilms, Nature **523**, 550 (2015).

[S4] J. Humphries, L. Xiong, J. Liu, A. Prindle, F. Yuan, H.A. Arjes, L. Tsimring, and G.M. Süel, Species-independent attraction to biofilms through electrical signaling, Cell **168**, 200 (2017).

[S5] J. Schindelin, I. Arganda-Carreras, E. Frise, V. Kaynig, M. Longair, T. Pietzsch, S. Preibisch, C. Rueden, S. Saalfeld, B. Schmid, J.-Y. Tinevez, D.J. White, V. Hartenstein, K. Eliceiri, P. Tomancak, and A. Cardona, Fiji: an open-source platform for biological-image analysis, Nature Methods **9**, 676 (2012).

[S6] R. P. Brent, *Algorithms for Minimization Without Derivatives* (Prentice-Hall Inc. 1973).

[S7] C. Picioreanu, F. Blauert, H. Horn, and M. Wagner, Determination of mechanical properties of biofilms by modelling the deformation using optical coherence tomography, Water Res. **145**, 588-598 (2018).

[S8] A.E. Ismail, G.S. Grest, D.R. Heine, and M. J. Stevens, Interfacial Structure and Dynamics of Siloxane Systems: PDMS-Vapor and PDMS-Water, Macromolecules **42**, 3186-3194 (2009).